International Journal of Microwave and Wireless Technologies

cambridge.org/mrf

Hybrid sparse array design using Delaunay Triangulation and Convex optimization for wide beam steering

Pan Gao[1] and Zhongquan Chen[2]

[1]Electrical Engineering Department, Eindhoven University of Technology, Eindhoven, The Netherlands and [2]Mathematics and Computer Science Department, Eindhoven University of Technology, Eindhoven, The Netherlands

Research Paper

Cite this article: Gao P, Chen Z (2025) Hybrid sparse array design using Delaunay Triangulation and Convex optimization for wide beam steering. *International Journal of Microwave and Wireless Technologies* **17**(3), 409–417. https://doi.org/10.1017/S1759078725000352

Received: 14 May 2024
Revised: 25 February 2025
Accepted: 8 March 2025

Keywords
beam steering; Convex; Delaunay Triangulation; grating lobes; hybrid; sparse array; side-lobe-level

Corresponding author: Pan Gao;
Email: pangao1125@gmail.com

Abstract

In this paper, we propose a hybrid sparse array design utilizing Delaunay Triangulation algorithm for element positioning and Convex algorithm for element excitation optimization. This Delaunay Triangulation algorithm yields a radiation pattern devoid of grating lobes. Then Convex algorithm is used to optimize the element excitations to further decrease side-lobe-level. The minimum inter-element distance is as large as 8 times of wavelength. The peak-side-lobe-level can be −17.3 dB. Furthermore, beam steering can be achieved with good performance within 80° field-of-view range.

Introduction

In recent years, sparse array has been widely used to optimize the beamforming in antenna array design [1–15]. Sparse array is obtained by reducing the number of radiating elements in an array. Compared to periodic array with the same aperture, sparse array can save a large amount of elements, significantly decreasing the manufacture cost and system complexity.

In addition to the element number, the distance between adjacent elements is a critical factor to consider. In certain applications, the dimensions of elements and the required spacing between them necessitate an inter-element distance larger than half of wavelength (0.5λ). Beyond this threshold, grating lobes are generated, leading to power dispersion and interference in undesired directions [16–18]. Consequently, distributing an array with a periodic configuration without the presence of grating lobes becomes unfeasible when the inter-element distance exceeds 0.5λ.

To address these challenges, sparse arrays offer a solution by allowing for the use of larger inter-element distances in array design without the occurrence of grating lobes. Various optimization techniques have been proposed, including particle swarm optimization (PSO) algorithm [19], genetic algorithm (GA) [20, 21], and Convex optimization [22, 23]. Through optimization of the element distribution, the peak-side-lobe-level (PSLL) of the array can be effectively minimized, while the grating lobes can be suppressed. However, the inter-element distance is still maintained not above the wavelength. Therefore, more investigations should be done for the situations where the inter-element distance is above the wavelength.

In addition to the aforementioned optimization algorithms, an alternative approach involves initially establishing a random element distribution in the array and subsequently adjusting the positions of elements. This process continues until the desired side-lobe-level (SLL) for the entire antenna array is achieved. Then the adjustment of element positions ceases.

In this paper, a two-dimensional (2D) sparse array is proposed employing Delaunay Triangulation coupled with Convex optimization. Delaunay Triangulation algorithm is utilized to distribute element positions, and Convex algorithm is utilized to optimize element excitations. What is more, the array maintains a minimum inter-element distance of up to 8λ, yielding a PSLL of −17.3 dB in 180 planes. Furthermore, this array can achieve beam steering with good performance within a field-of-view range of 80°.

Compared with some existing sparse array designs, there are several benefits and advantages for the design in this paper. First, some traditional methods, such as GA in paper [20] and PSO algorithm in paper [19], always work on arrays with smaller inter-element distance (not beyond half of wavelength). The main purpose of the designs is to decrease the element number. When the inter-element distance is beyond half of wavelength, these methods cannot prevent

© The Author(s), 2025. Published by Cambridge University Press in association with The European Microwave Association.

the appearance of grating lobes. However, our design can obtain radiation pattern with no grating lobe and low SLL when the minimum inter-element distance is as large as 8λ. Second, low PSLL is another advantage of this design. The PSLL in this paper is suppressed to lower level of −17.3 dB, compared with the design with a smaller minimum inter-element distance of λ in paper [24], which owes a PSLL of −7.5 dB. The combination of the Delaunay Triangulation and Convex optimization provides more flexibility in the suppression of both SLL and grating lobes, due to the optimization on both array configuration and element excitations. Third, the Delaunay Triangulation algorithm can generate a desirable sparse configuration using significantly less computation and time, compared with the complex design process in papers [25, 26]. Besides, wide beam steering is an additional advantage of this design method.

Submission proposed algorithm for sparse array design

Array configuration with Delaunay Triangulation algorithm

According to antenna theory, the radiation pattern of the antenna array is defined by element pattern (EP) and array factor (AF). Consider a planar antenna array with $M\times N$ identical elements, with identical amplitude and initial null phase.

Assuming the EP is $f(\theta)$, the radiation pattern of the planar array can be obtained from the multiplication of AF and EP. The radiation pattern can be expressed as follows:

$$E(\theta,\phi)=\sum_{m=1}^{M}\sum_{n=1}^{N}\alpha_{m,n}\exp\{j[(m-1)(kd_x\sin\theta\cos\phi)+(n-1)(kd_y\sin\theta\sin\phi)]\}f(\theta) \quad (1)$$

Here, d_x and d_y are the inter-element distances in x- and y-axis, respectively; $k=2\pi/\lambda$ is the wave number at the working wavelength λ. $\alpha_{m,n}$ represents the excitation of the element in mth position in the x-direction, and the nth position in the y-direction. The excitation of all elements is denoted by a vector:

$$\boldsymbol{\alpha}=(\alpha_{1,1},\alpha_{1,2},\dots\dots,\alpha_{m,n},\dots\dots,\alpha_{M,N})^T \quad (2)$$

The PSLL is defined in equation (3), where θ_0 is the main beam angle:

$$PSLL=\max\{|E(\theta)/E(\theta_0)|\} \quad (3)$$

The array distribution design is accomplished by a controlled random movement of elements. In the beginning, the initial points with the specified number are randomly generated within the required square region. Then boundary points are defined and interpolated to form a smooth boundary. The repulsion mechanism is applied iteratively to prevent the points from becoming too close, adjusting their positions based on the repulsive force calculated from the Delaunay triangulation and distances between points. The configuration of the elements adheres to the constraint of the minimum inter-element distance, hence termed a pseudorandom configuration. The positions of elements are updated each time in the loop based on the repulsion force. Finally, the updated positions of elements are plotted, generating the sparse array configuration.

Delaunay Triangulation is a geometric algorithm for dividing a set of points in a plane into a non-overlapping triangle mesh that satisfies a specific optimality criterion [27]. The Delaunay Triangulation of a set of points has the property that no point lies within the circumcircle of any triangle in the mesh. The key characteristic of Delaunay Triangulation is that it maximizes the minimum angle of all the triangles in the mesh, leading to more regular and well-conditioned triangles. This property makes Delaunay Triangulation desirable in certain applications, due to more geometrically favorable triangular meshes produced.

To construct a sparse array, Delaunay Triangulation is applied to establish a mesh or connectivity structure for the populated elements in an array. The points representing elements are linked in a manner uploading the empty circumcircle property. This strategy leverages the inherent property of Delaunay Triangulation, including the optimal triangle quality and the assurance of geometrically advantageous connectivity between these elements.

Delaunay Triangulation can maximize the minimum angle of all the angles and minimize the edge length variance in the triangles, which are composed by any three points in the array plane. This leads to more uniform spacing between the element positions. It can ensure that the groups of points in the array plane are not tightly packed. Therefore, the distribution of elements can be ensured to meet the requirement of minimum inter-element distance.

Excitation optimization with Convex algorithm

Based on the sparse distribution obtained from the Delaunay Triangulation in the first step, Convex optimization [28] is utilized to optimize the excitations of the elements in this sparse array.

Convex algorithm is utilized to minimize the norm of the excitation vector, l_1-norm. This method is based on compressive sensing theory, aiming to minimize the number of samples to reconstruct a signal. In this optimization process, a desired mask level *MaskLevel* is proposed as the additional constraint for selection of proper solutions. In details, the program performs continuous iterations until the SLL reaches the mask level.

$$\begin{aligned}&\min\|\boldsymbol{\alpha}\|_1\\&E(\theta_0)=1\\&subject\ to\ E\le 10^{MaskLevel/20}\end{aligned} \quad (4)$$

In the initial array distribution, all elements are excited with a value of 1. Here, SDPT3 solver is applied in Convex algorithm. SDPT3 solver is one of the default solvers in Convex, which supports all the continuous (non-integer) models. With this solver, in the Convex optimization, the excitations of elements are allowed to be non-integer value. Subsequently, after Convex optimization on the element excitations, a new set of excitation values is generated. The positions of the elements in the array remain unchanged from the initial configuration.

Procedure of the hybrid algorithm

Figure 1 presents the flow diagram of the design process. By employing the Delaunay Triangulation algorithm, the positions of the elements are adjusted while adhering to both the minimum inter-element distance and the desired radiation pattern constraints. In this workflow, Delaunay Triangulation plays a crucial role in managing point repulsion, ensuring that the points are adequately spaced and not too proximate to one another. Once the optimal element position set is achieved, the adjustment of element positions within the array ceases. Then, Convex algorithm is operated on the excitation vector of these elements. In the beginning of the optimization process, a certain value of the PSLL is defined and

https://doi.org/10.1017/S1759078725000352 Published online by Cambridge University Press

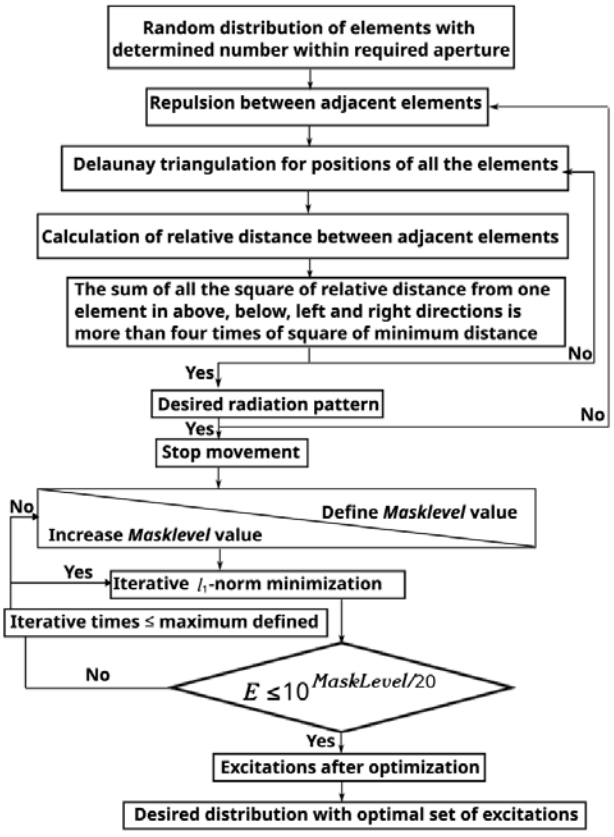


Figure 1. Flow diagram of the sparse array design.

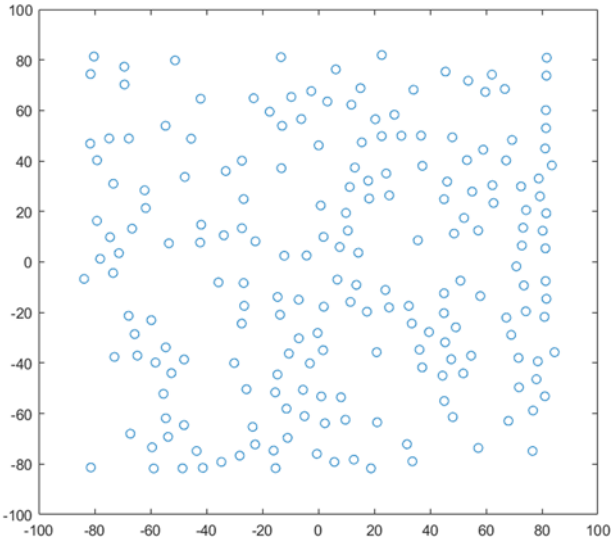


Figure 2. Distribution of the 2D sparse array.

tried with this optimization algorithm. If no solution is found after the maximum iteration time, the PSLL value is changed to another one. Until the radiation pattern fitting the given mask is obtained, the optimization process ceases. Finally, a sparse distribution and an optimal set of excitations of elements are achieved by this hybrid optimization.

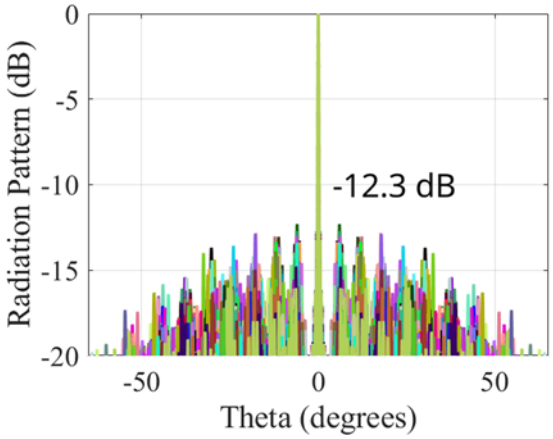


Figure 3. Radiation pattern of the sparse array with optimal configuration in 180 planes.

Array configuration and radiation pattern

In the antenna array, each element is a broadside antenna, whose maximum radiation directs normal to the axis of the array. We assume the radiating pattern of each element (EP) is Gaussian pattern with a full-width at half-maximum of 75°.

In this configured array, the desired half-power beam width (HPBW) of the main lobe is set at 0.3°. The square planar array spans a length of 169λ. In a periodic array with an inter-element distance of 0.5λ, achieving an HPBW of 0.3° would necessitate a total of 338×338 elements in the array.

Taking into account the need for larger-sized elements, we establish a minimum distance of 8λ between adjacent elements. Following optimization, the array consists of 202 elements. Here, the coordinate values are expressed in terms of multiples of the wavelength. In Fig. 2, the center of each blue circle denotes the exact position of an element, and the element-to-element distance is measured from center to center.

Figure 3 displays the radiation pattern of the antenna array across all 180 (from 0° to 180°with 1° as increment) ϕ-planes. Notably, no grating lobes are observed in this radiation pattern. The PSLL in all 180 ϕ-planes remains below −12.3 dB. These outcomes affirm that the pseudorandom distribution effectively suppresses both grating lobes and side lobes.

Figure 4 illustrates the 2D radiation pattern. The HPBW of the main lobe measures 0.3°. Given the small HPBW, the main lobe segment is enlarged and positioned in the left corner of the figure. This approach, utilizing 8λ inter-element distance, provides ample room for larger-sized elements. This stands in contrast to array designs employing optimization algorithms with 0.5λ or 0.6λ inter-element distances as reported in papers [19–21]. While these optimization algorithms yield lower PSLL due to their smaller inter-element distances, their performance tends to diminish as the inter-element distance increases. In contrast, in this instance, the inter-element distance can extend up to 8λ. This represents a clear advantage over previous optimization methods.

As comparison, a periodic square array with an identical aperture and inter-element distance (8λ) is simulated. Theoretically, its main lobe should exhibit the same beam width as that of the pseudorandom array. The radiation pattern of the periodic array is depicted in Fig. 5. As observed, grating lobes emerge in various directions, leading to power dispersion and undesirable interference. When steering toward different directions, the range

https://doi.org/10.1017/S1759078725000352 Published online by Cambridge University Press

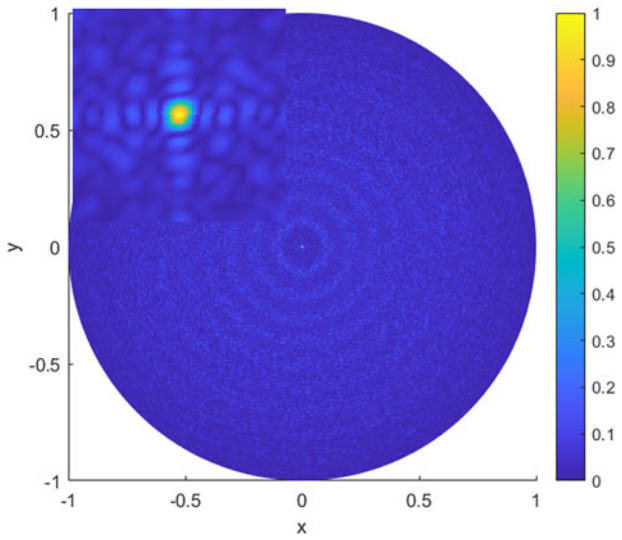


Figure 4. Radiation pattern of the sparse array ($x = \sin\theta\cos\phi$, $y = \sin\theta\sin\phi$. *Note*: The main beam is enlarged and put in the left corner of the figure).

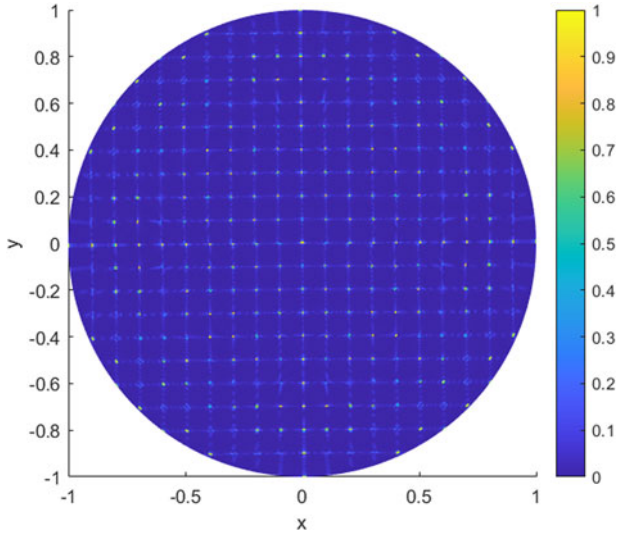


Figure 5. Radiation pattern of the periodic array with the same aperture.

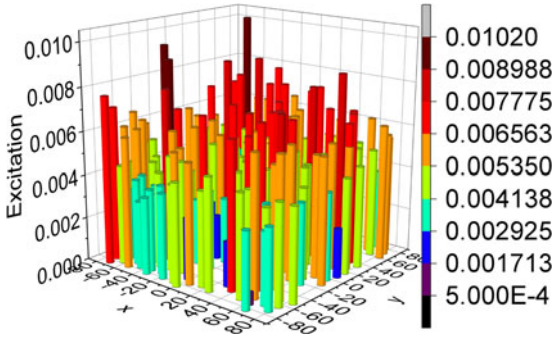


Figure 6. Excitation of each element in each position in this sparse array.

of steering is constrained by the presence of grating lobes. These drawbacks collectively render periodic arrays less favorable for practical applications.

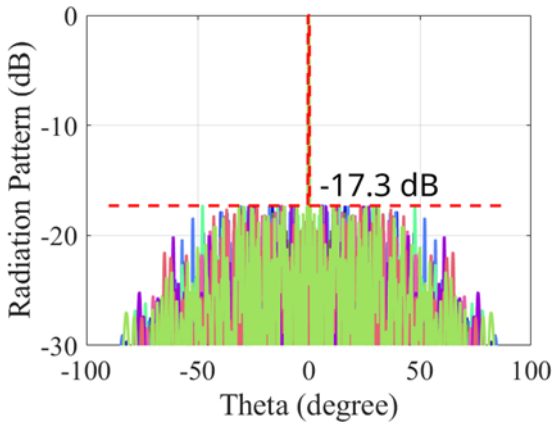


Figure 7. Radiation pattern of the sparse array after Convex optimization.

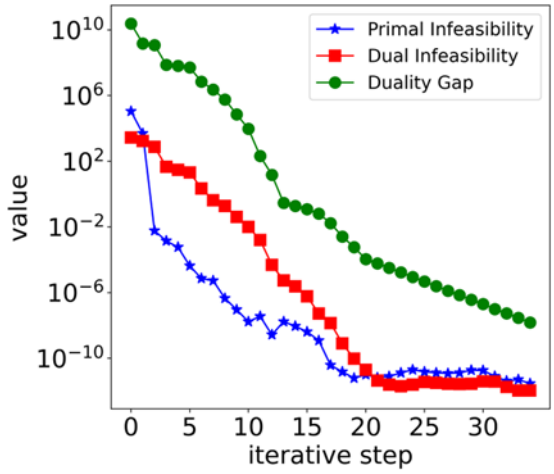


Figure 8. The values of primal infeasibility, dual infeasibility, and duality gap at each iterative step during the optimization process.

Figure 6 displays the excitation values for all the elements in the sparse array, while the positions of the elements in the array remain unchanged from the initial configuration. The primary contribution of the excitation optimization is the notable reduction in PSLL. As depicted in Fig. 7, a PSLL of −17.3 dB is attained, which is 5 dB lower than the pre-optimized PSLL shown in Fig. 3. This significant reduction in PSLL underscores the effectiveness of the optimization on the element excitations.

In Convex optimization, the SDPT3 solver employs a path-following algorithm to achieve convergence. This approach ensures a balanced maintenance of both primal and dual feasibility while effectively minimizing the duality gap. The convergence process is monitored using three primary indicators: primal infeasibility, dual infeasibility, and duality gap. The convergence criterion is defined as the maximum of these indicators being less than 1.5×10^{-8} to ensure accuracy. The evolution of these indicators throughout the optimization process is illustrated in Fig. 8. This figure demonstrates that the convergence criteria are satisfied after 34 iterations, resulting in a small duality gap of 1.5×10^{-8}. The relative primal and dual infeasibility are 2.9×10^{-13} and 1.1×10^{-12}, respectively.

https://doi.org/10.1017/S1759078725000352 Published online by Cambridge University Press

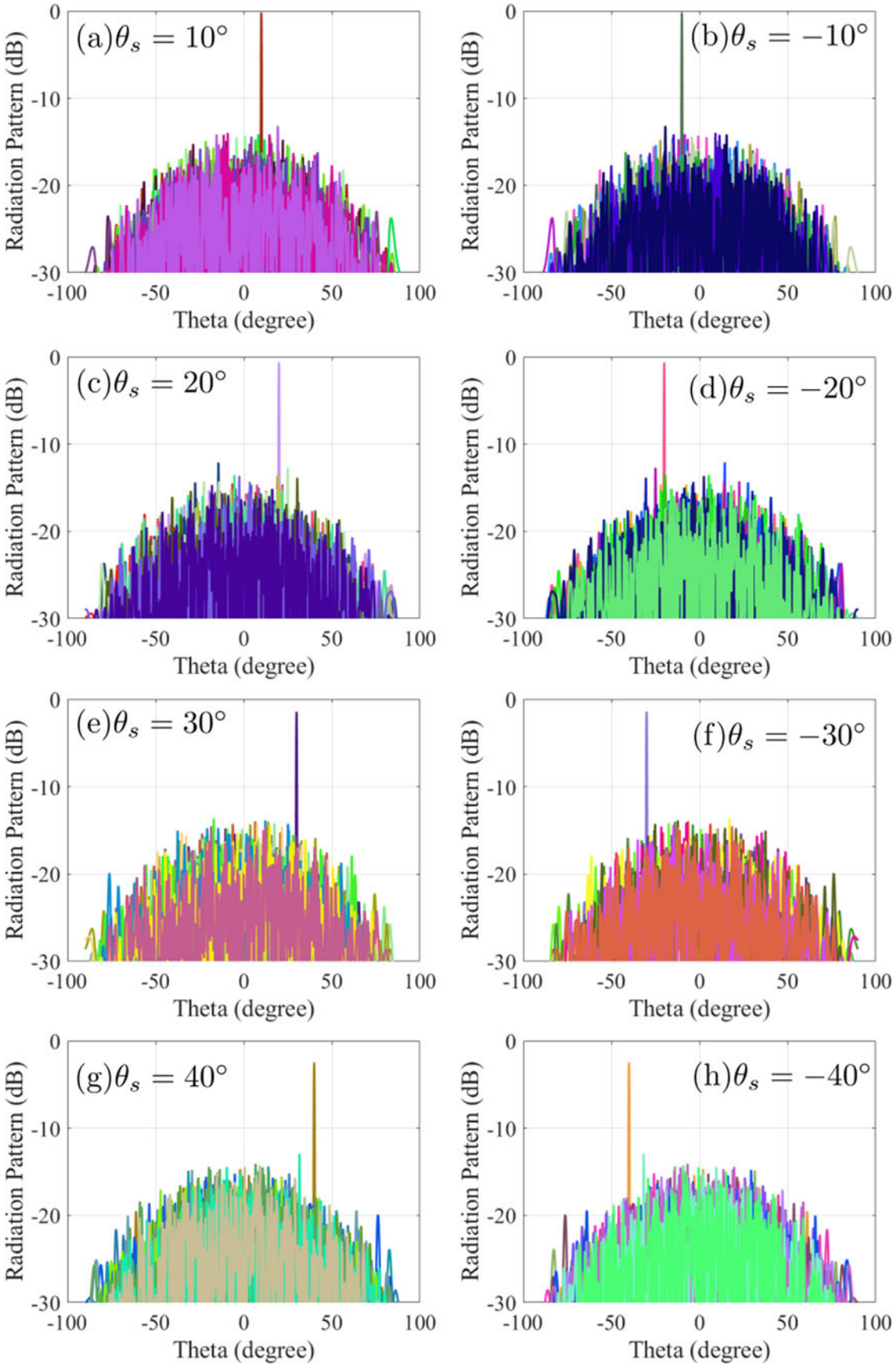


Figure 9. Radiation pattern in E plane when the steering angle is (a) 10°; (b) −10°; (c) 20°; (d) −20°; (e) 30°; (f) −30°; (g) 40°; (h) −40°.

https://doi.org/10.1017/S1759078725000352 Published online by Cambridge University Press

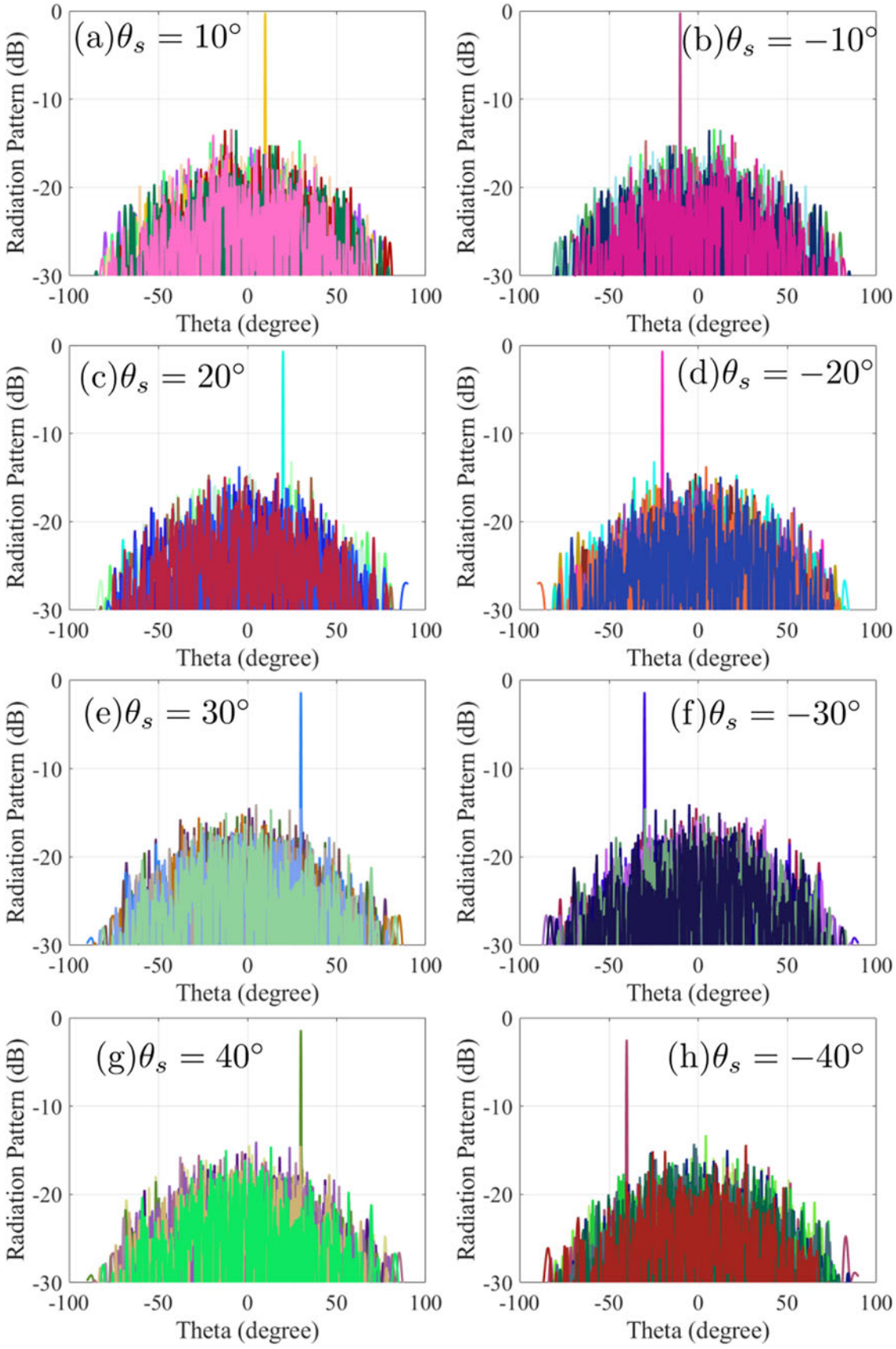


Figure 10. Radiation pattern in D plane when the steering angle is (a) 10°; (b) −10°; (c) 20°; (d) −20°; (e) 30°; (f) −30°; (g) 40°; (h) −40°.

https://doi.org/10.1017/S1759078725000352 Published online by Cambridge University Press

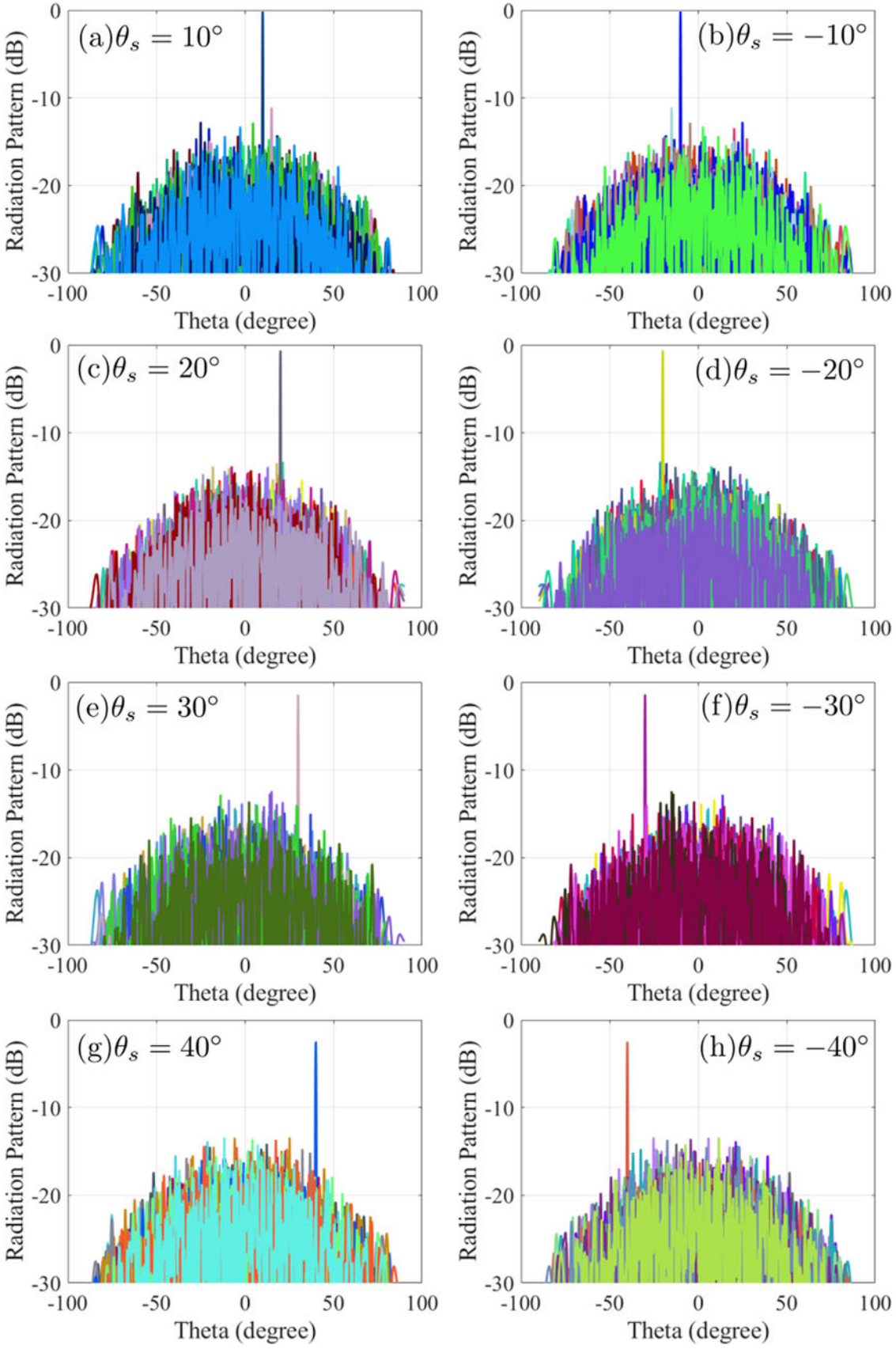


Figure 11. Radiation pattern in H plane when the steering angle is (a) 10°; (b) −10°; (c) 20°; (d)–20°; (e) 30°; (f) −30°; (g) 40°; (h) −40°.

https://doi.org/10.1017/S1759078725000352 Published online by Cambridge University Press

Beam steering performance

Beam steering is an important feature to investigate the effectiveness of array design [29–31]. Using the same array distribution and element excitations derived from the broadside pattern, we add different phases to steer the main lobe toward various directions within the range of (−40° to 40°). The radiation patterns of this sparse array when steering toward 10°, −10°, 20°, −20°, 30°, −30°, 40°, −40° in E plane, D plane, and H plane are shown in Figs. 9–11, respectively.

The radiation patterns of the sparse array demonstrate excellent performance when the beam is steered toward all of these directions. The effective beam steering, characterized by low SLL within a wide field of view, is attributed to the entirely random design of the array configuration and the appropriate excitation optimization of the elements.

The radiation pattern results indicate the effectiveness of this hybrid design method. Grating lobes are avoided and low SLL are achieved while much fewer elements are used in the array plane. In addition, beam steering can be operated within 80° field-of-view range, which provides a solution for wide-range scanning applications. Compared with uniform array, the reduction of number of elements is an obvious advantage. The avoidance of grating lobes decreases power consumption and interference from other directions, increasing the efficiency and detection accuracy. Compared with some conventional sparse array design methods, such as PSO algorithm, GA, this design method can work on the arrays with larger inter-element distance (larger than half of wavelength). According to antenna theory, when the inter-element distance is or below half of wavelength, no grating lobe appears in radiation pattern. When the inter-element distance is beyond half of wavelength, the grating lobes appear in the radiation pattern. Thus, these methods are not able to achieve good radiation without the interference of grating lobes. However, our design can solve this problem. In addition to the avoidance of grating lobes, low level of PSLL can be achieved. Furthermore, the Delaunay Triangulation algorithm employed in this design can generate a sparse array with less calculation and time cost than some complex design methods [25, 26].

The main contribution of the design method proposed in this paper is to provide possibility for sparse array applications where large-size elements are applied. The element number is significantly reduced. Therefore, the desired radiation pattern can be achieved with less cost and power consumption. The system complexity will also be reduced. Besides, larger distance between elements reduces mutual coupling among adjacent elements. For some antenna applications requiring high resolution and wide beam steering, this design can provide solution to solve these problems with less complexity and cost.

Conclusion

In conclusion, a hybrid design methodology based on Delaunay Triangulation and Convex optimization is proposed for planar sparse array design. In this design, Delaunay Triangulation algorithm is utilized to distribute the positions of elements and Convex algorithm is utilized to optimize the excitations of elements. Radiation pattern devoid of grating lobes and featuring low SLL can be achieved with a limited number of elements with a minimum inter-element distance of 8λ. This approach offers a distinct advantage in the form of large minimum inter-element distance. In comparison to periodic array, the reduction in the number of elements leads to lower power consumption and simplified manufacturing process. In addition, beam steering can be achieved with good performance within 80° field-of-view range.

Competing interests. The authors declare no conflicts of interest.

References

1. **Cen L, Ser W, Yu ZL and Rahardja S** (2008) An improved genetic algorithm for aperiodic array synthesis. *IEEE International Conference on Acoustics, Speech, and Signal Processing* 2465–2468.
2. **Jarske P, Saramaki T, Mitra SK and Neuvo Y** (1988) On properties and design of nonuniformly spaced linear arrays. *IEEE Transactions on Signal Processing* **36**, 372–380.
3. **Skolnik M, Nemhauser G and Sherman JI** (1964) Dynamic programming applied to unequally spaced arrays. *IEEE Transactions on Antennas and Propagation* **12**, 35–43.
4. **Chen K, He Z and Han C** (2006) A modified real GA for the sparse linear array synthesis with multiple constraints. *IEEE Transactions on Antennas and Propagation* **54**, 2169–2173.
5. **Oliveri G and Massa A** (2011) Genetic algorithm (GA)-enhanced almost difference set (ADS)-based approach for array thinning. *IET Microwaves Antennas and Propagation* **5**, 305–315.
6. **Zhang S, Gong SX, Guan Y, Zhang PF and Gong Q** (2009) A novel IGA-EDSPSO hybrid algorithm for the synthesis of sparse arrays. *Progress in Electromagnetic Research* **89**, 121–134.
7. **Panduro MA** (2006) Design of non-uniform linear phased arrays using genetic algorithms to provide maximum interference reduction capability in a wireless communication system. *Journal of the Chinese Institute of Engineers* **29**, 1195–1201.
8. **Panduro MA, Mendez AL, Dominguez R and Romero G** (2006) Design of non-uniform circular antenna arrays for side lobe reduction using the method of genetic algorithms. *AEU - International Journal of Electronics and Communications* **60**, 713–717.
9. **Panduro MA and Brizuela CA** (2008) Evolutionary multi-objective design of non-uniform circular phased arrays. *COMPEL - The International Journal for Computation and Mathematics in Electrical and Electronic Engineering* **27**, 551–566.
10. **Panduro MA** (2007) Design of coherently radiating structures in a linear array geometry using genetic algorithms. *AEU - International Journal of Electronics and Communications* **61**, 515–520.
11. **Panduro MA, Brizuela CA, Covarrubias D and Lopez C** (2006) A trade-off curve computation for linear antenna arrays using an evolutionary multi-objective approach. *Soft Computing* **10**, 125–131.
12. **Reyna Maldonado A, Panduro MA, Del Rio Bocio C and Mendez AL** (2013) Design of concentric ring antenna array for a reconfigurable isoflux pattern. *Journal of Electromagnetic Waves and Applications* **27**, 1483–1495.
13. **Ibarra M, Panduro MA, Andrade ÁG and Reyna A** (2015) Design of sparse concentric rings array for LEO satellites. *Journal of Electromagnetic Waves and Applications* **29**, 1983–2001.
14. **Panduro MA, Reyna A and Covarrubias DH** (2019) Non-uniform concentric rings design for ultra-wideband arrays. *Sensors* **19**, 2262.
15. **Reyna Maldonado A and Panduro MA** (2015) Synthesis of concentric ring antenna array for a wide isoflux pattern. *International Journal of Numerical Modelling: Electronic Networks, Devices and Fields* **28**, 433–441.
16. **W. Alshrafi W, Bassam A and D. Heberling D** (2020) Grating lobe mitigation in series-fed patch periodic leaky-wave antenna using parasitic monopoles. *IEEE Antennas and Wireless Propagation Letters* **19**, 2472–2476.
17. **Bogaerts W, Dwivedi S, Jansen R, Rottenberg X and Dahlem MS** (2020) A 2D pixelated optical beam scanner controlled by the laser wavelength. *IEEE Journal of Quantum Electronics* **27**, 1–12.
18. **Bogaerts W, Dahlem M, Dwivedi S, Jansen R and Rottenberg X** (2020) Dispersive optical phased array circuit for high-resolution pixelated 2D far-field scanning controlled by a single wavelength variable. *Proceedings*

https://doi.org/10.1017/S1759078725000352 Published online by Cambridge University Press

Smart Photonic and Optoelectronic Integrated Circuits XXII **11284**, 119–133.
19. **Chen T, Dong Y, Jiao Y and Zhang F** (2006) Synthesis of circular antenna array using crossed particle swarm optimization algorithm. *Journal of Electromagnetic Waves and Applications* **20**, 1785–1795.
20. **Kwon G, Park J, Kim D and Hwang KC** (2017) Optimization of a shared-aperture dual-band transmitting/receiving array antenna for radar applications. *IEEE Transactions on Antennas and Propagation* **65**, 7038–7051.
21. **Enache F, Deparateanu D, Enache A and Popescu F** (2016) Sparse array antenna design based on Dolph-Chebyshev and genetic algorithms, Proceedings of the International Conference on Electronics, Computers and Artificial Intelligence, IEEE, 1–4.
22. **Yang SJ, Young DK, Dong WY and Myung NH** (2018) Antenna modeling using sparse infinitesimal dipoles based on recursive convex optimization. *IEEE Antennas and Wireless Propagation Letters* **17**, 662–665.
23. **Dong X, Li H, Tan J, Hu J and Jiang Y** (2021) A PSO-CVX algorithm of sum and difference beam patterns for time-modulated antenna array. *International Journal of Antennas and Propagation* **2021**, 1–9.
24. **Alidoustaghdam H, Kokkeler A and Miao Y** (2022) Multibeam Sparse Tiled Planar Array for Joint Communication and Sensing. *arXiv* **2209**, 08847.
25. **Zhang H, Bai B, Zheng J and Zhou Y** (2020) Optimal design of sparse array for ultrasonic total focusing method by binary particle swarm optimization. *IEEE Access* **8**, 111945–111953.
26. **Mo H, Tong Y, Wang Y, Wang K, Luo D and Li W** (2023) Sparse non-uniform linear array-based propagator method for direction of arrival estimation. *Electronics* **12**, 3755.
27. **Delaunay B, Vide S, Lamémoire A and De Georges V** (1934) Bulletin de l'Academie des Sciences de l'URSS. *Class of Mathematical and Natural Sciences* **6**, 793–800.
28. **Boyd S, Boyd SP and Vandenberghe L** (2004) *Convex Optimization*, Cambridge, UK: Cambridge university press.
29. **Panduro MA and Del Rio C** (2009) Design of beam-forming networks using CORPS and evolutionary optimization. *AEU - International Journal of Electronics and Communications* **63**, 353–365.
30. **Juárez E, Mendoza MAP, Covarrubias DH, Maldonado AR, Sanchez B and Del Rio C** (2021) An innovative way of using coherently radiating periodic structures for phased arrays with reduced number of phase shifters. *IEEE Transactions on Antennas and Propagation* **70**, 307–316.
31. **Reyna Maldonado A and Panduro MA** (2008) Optimization of a scannable pattern for uniform planar antenna arrays to minimize the side lobe level. *Journal of Electromagnetic Waves and Applications* **22**, 2241–2250.



Pan Gao is PhD in Electrical Engineering department in Eindhoven University of Technology. She received Master degree from Chinese Academy of Sciences on optical engineering. She works on optical phased array, sparse array and laser.



Zhongquan Chen is currently a PhD candidate at the Eindhoven University of Technology, focusing on multiscale modeling of network dynamics. His Master's work focused on statistical mechanics at the University of Saskatchewan in 2017.

https://doi.org/10.1017/S1759078725000352 Published online by Cambridge University Press